320 to 480 meV when raising the temperature from room temperature to 550 °C. The change is of the same order as the observed increase in the width of band (1) in the spectrum of methyl vinyl sulfide and is thus much smaller than the found change connected with the occurrence of the new band (2a) in the same spectrum.

(18) It is interesting to note that the values $\Delta E_0^0 r = -2.4 \pm 0.2$ kcal/mol and $Q^0_{cis}/Q^0_{gauche} = 0.3 \pm 0.1$ as derived from eq 2 agree, within the limits of error, with those derived from eq 3. Equation 1 cannot be used because the changes in the $I_{③}/I_{②}$ values (see Table I) are insignificant when compared to the experimental errors involved.

Isotopically Selective Spectroscopy and Photochemistry of *s*-Tetrazine in Crystals and Mixed Crystals at Low Temperature[1]

R. M. Hochstrasser* and D. S. King

Contribution from the Department of Chemistry and Laboratory for Research on the Structure of Matter, The University of Pennsylvania, Philadelphia, Pennsylvania 19174. *Received February 9, 1976*

Abstract: The high resolution $^1B_{3u}(n\pi^*)$–^1A_g absorption, single isotopic fluorescence, and single isotopic fluorescence excitation spectra of normal *s*-tetrazine and the ^{15}N, ^{13}C, and D monosubstituted *s*-tetrazines in natural abundance in benzene at 1.6 K; the photophysics and photochemistry of *s*-tetrazine in solution (300 K) and solid (4.2 to 1.6 K); and the laser isotope enrichment of *s*-tetrazine in mixed crystals (1.6 K) are reported and discussed. All spectra were dominated by the single promoting mode $\nu_{6a}(a_g)$. The zero-point state energy of the $^1B_{3u}(n\pi^*)$ transition of normal, $^{15}N_1$, $^{13}C_1$, and D_1 tetrazine is 17 233.9, 17 236.9, 17 237.5, and 17 241.7 cm^{-1}; $\nu_{6a''}$ is 727.3, 723.2, 720.2, and 717.9 cm^{-1}; and $\nu_{6a'}$ is 702.5, 695.3, 683.9, and 677.2 cm^{-1}, respectively. The fluorescence lifetime in benzene (300 K) is 450 ± 55 ps corresponding to a quantum yield of 1.1×10^{-3}. In solution (300 K) and solid (1.6 K) the fluorescence quantum yield is constant throughout the region of appreciable absorption strength. There is *no* observable intersystem crossing. The triplet $[(^3B_{3u}(n\pi^*)]$ pumped phosphorescence quantum yield is ca. 0.5×10^{-3}. The predominant depopulating mechanism of both the $^1B_{3u}$ and $^3B_{3u}$ states of *s*-tetrazine is a photoenhanced decomposition. This reaction shows marked spin selectivity $[k(^1B_{3u})/k(^3B_{3u}) = 2.1 \times 10^5]$ and proceeds, even in mixed crystals at 1.6 K, to produce directly the stable products $N_2 + 2HCN$ quantitatively. Samples of ^{15}N and ^{13}C monosubstituted *s*-tetrazine (in benzene) were purified from natural abundance by a laser isotope separation and purification scheme in the solid at 1.6 with enrichment factors of 10^4. Mixtures of enriched photoproducts were also produced.

I. Introduction

Recently there have been exposed some unique photochemical properties of the molecule *s*-tetrazine.[2] Following excitation with visible light the stable molecules HCN and N_2 are produced with high quantum yield. This reaction is the reverse of the structurally analogous classic acetylene condensation to produce benzene. A main objective of our study was to try to understand the reaction mechanism and the extent to which it can be related to the electronic structure and nonradiative properties of the photoexcited states. Another aspect of our study concerns laser-induced separation of isotopes, since in cases such as *s*-tetrazine many of the features required for efficient separation are present. These include low energy absorption spectra that are readily accessible by visible lasers; stable photoproducts that do not undergo efficient isotopic exchange reactions; a high photochemical quantum yield; and finally, the existence of substantial isotope shifts for C, N, and H atoms. These isotope shifts arise because the electronic excitation involves changes in the electronic distribution around all the atoms in the molecule.

We have shown in our earlier work that the photochemical decomposition of *s*-tetrazine can also be brought about in molecular mixed crystals at 1.6 K, thereby introducing the reality of studying single vibronic level photochemistry in low-temperature solids. In the present paper a detailed assessment of this general approach will be given.

The photophysical properties of azines have been extensively studied both in the condensed and gaseous phases. They all have $n\pi^*$ states, singlets and triplets, that are frequently intermeshed with the $\pi\pi^*$ states of benzene parentage. The radiationless processes that occur after excitation follow no general course: they often appear to be medium induced, and in the condensed phase intersystem crossing is frequently an efficient process. Knight and Parmenter[3] have recently summarized the data available for dilute gases of the azines. Until recently it was thought that the azines were relatively stable to light absorption into their lowest energy states. *s*-Tetrazine is clearly not stable in visible light,[2,4,5] and gaseous pyridazine was recently shown to produce N_2 with a quantum yield of 0.12 following excitation to its lowest $n\pi^*$ singlet state.[6] Thus it is clear that even after considerable experimental and theoretical effort beginning in the early 50's,[7,8] the azines continue to pose interesting and unanswered questions regarding both their physical and chemical behavior.

Two excited electronic states of *s*-tetrazine in the 4000–8000-Å region have been characterized: these are the $^1B_{3u} \leftarrow {}^1A_g$ and $^3B_{3u} \leftarrow {}^1A_g$ transitions both of which consist mainly of a progression of a 700 cm^{-1} vibrational mode, 6a. A further absorption occurs in the region of 3000 Å and this has been assumed to correspond to an $n \rightarrow \pi^*$ transition. Following the synthesis of *s*-tetrazine in 1906 by Curtius[9] and the observation of sharp line spectra in the gas by Koenigsberger and Vogt[10] the spectroscopy of tetrazine was extensively studied in the vapor,[10-13] solutions,[14,15] and in crystalline and mixed crystalline systems at low temperatures.[4,5,15,16] Recently attention was focused on the kinetics of the radiative[4,5,17,18] and nonradiative[2] processes that tetrazine undergoes in various media.

II. Experimental Methods

(1) Materials and Sample Preparation. *s*-Tetrazinedicarboxylic acid was synthesized by the method of Spencer, Cross, and Wiberg.[11] For the neat and mixed crystal work a stockpile of *s*-tetrazine was prepared

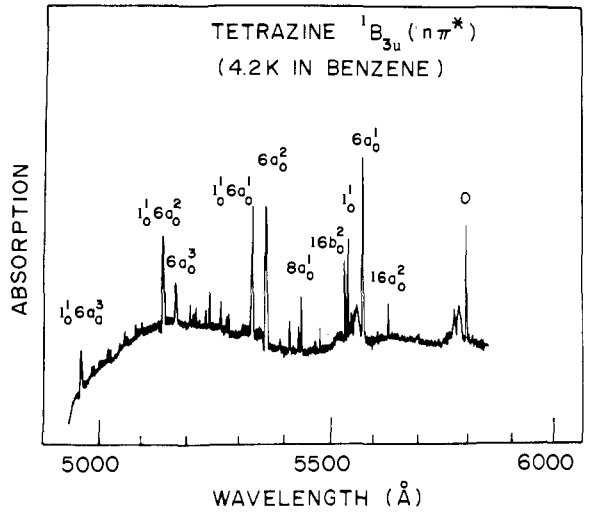

Figure 1. The $^1B_{3u}$–^1A_g absorption spectrum of *s*-tetrazine in benzene at 4.2 K. The spectrum was photographed with 1-cm^{-1} resolution on a Baird 3-m spectrometer, using a Xe arc continuum background.

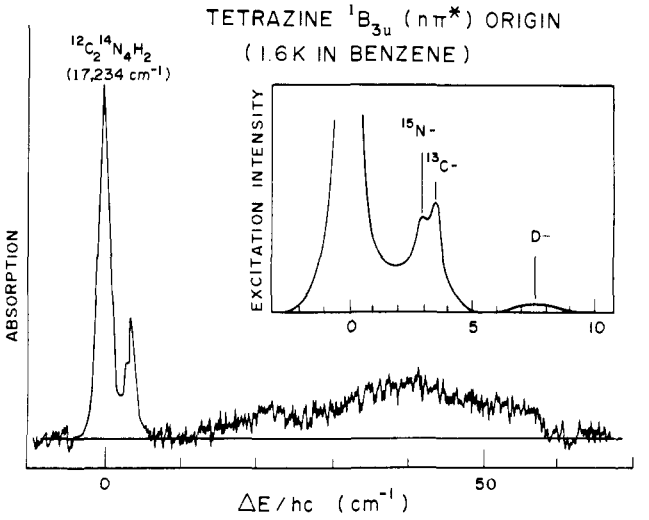

Figure 2. The absorption and fluorescence excitation spectra of the *s*-tetrazine singlet origin in benzene at 1.6 K. The absorption spectrum was photographed on a 3-m Baird spectrometer with 1-cm^{-1} resolution using a Xe continuum. The fluorescence excitation spectrum was obtained photoelectrically by monitoring the total fluorescence while scanning a 0.6-cm^{-1} N_2 pumped dye laser through the origin region.

by the bulk vacuum sublimation technique previously described.[4] The red microcrystals thus obtained were stored in vacuo and protected against thermal and photodecomposition until needed. Large single crystals of *s*-tetrazine were grown by gradient vacuum sublimation in a freezer by placing a small surface area of the storage bulb in direct contact with the cooling coils for a few days.

The small quantities of uncontaminated, unphotolyzed *s*-tetrazine required for the thin film photolysis studies at 4.2 K were synthesized on line just prior to deposition. A 1-to-5 mixture of *s*-tetrazinedicarboxylic acid and Cab-O-Sil 50 Å glass particles was finely ground in a mortar and placed in the reaction chamber (25 ml) of a small greaseless vacuum manifold connected via an O-ring stopcock and N_2 trap to an oil diffusion pump. The glass vacuum manifold, consisting of the sample chamber, cold trap, and isolating O-ring vacuum stopcocks, was warmed and evacuated to $< 10^{-4}$ Torr. The manifold was isolated from the pumping system, and the cold trap was immersed in liquid N_2 and a preheated (~220 °C) oil bath quickly raised to totally submerge the sample chamber. The reaction proceeded immediately and vigorously to completion within 30 s, all products being condensed in the nitrogen cold trap. The liquid nitrogen bath was then replaced with an ice bath and the evolved CO_2 pumped off. The tetrazine was then vacuum sublimed into a 2-l. bulb with a cold finger for efficient film deposition at room temperature. The yield in this small scale decarboxylation was about 50%.

The benzene used for our solution and mixed crystal work was Baker spectrograde. It was treated successively with concentrated H_2SO_4, distilled water, dilute NaOH, water, and $CaCl_2$. The final product was distilled over P_2O_5 prior to use. The mixed crystals were doped at 10^{-3} to 10^{-5} mol fraction and grown in the standard Bridgeman manner. Good single crystals with low rejection were obtained using normal crystal growth rates.

The neat tetrazine films were deposited onto a CsI optical cold finger from the room temperature vapor pressure of *s*-tetrazine (ca. 1 Torr) over a solid sample in the bulb. The cold finger was a part of a variable temperature cryostat in which the sample holder directly contacted liquid helium for cooling to 4.2 K.

The film deposition temperatures varied from 270 K > T > 4 K depending on the system and the spectral properties desired in our sample. Annealing at 200 K was found to improve the sample quality quite significantly as witnessed by the dramatic decrease in the inhomogeneous line widths of the spectra.

(2) **Spectroscopic Techniques.** Absorption spectra were recorded on a 3-m eagle mount Baird Atomic spectrometer. A 450 W Xe arc provided the background continuum and a 20 mA Fe–Ne hollow cathode lamp provided sharp lines for calibration purposes. Instrument slit widths of 50 μm gave spectral resolution of 1 cm^{-1} and several observed line widths are instrumentally limited. Kodak type 103-a-F plates were used with exposure times of typically 0.5 to 5 min.

Higher resolution spectra were obtained with a 2-m Jarrell Ash scanning spectrometer in 16th order. Again the 450 W Xe lamp and Fe–Ne hollow cathode provide the absorption background and calibration lines, a 50 μm slit width gave 0.1-cm^{-1} resolution. The spectra were recorded on 103-a-F Kodak plates.

The source used for selective excitations was a tunable dye laser pumped by a 100 KW Avco N_2 super-radiator. The dye laser cavity contains a partially reflecting mirror, a flowing dye cell with 6° windows, a 20× or a 40× beam expander, and a tunable Bausch and Lomb echelle grating with 316 grooves/mm and a 63° 26′ blaze angle. Rhodamine 6G, fluorescein, 7-dimethyl-4-ethylcoumarin, coumarin 102, coumarin 6, and various mixtures in ethanol were used for the active medium to give lasing from 6500 to 4500 Å.

The fluorescence was detected by a cooled Ga–As photomultiplier having nearly linear response from 4000 to 8000 Å and <1 nA anode dark current background at 1600 V cathode voltage. The fluorescence was observed either broad band through suitable colored glass filters to cut out the exciting laser light, or with selectivity through a scanning Spex monochromator with adjustable slits and a dispersion of 5 Å/mm. Typical slit widths varied from 200 to 20 μm for fluorescence and single isotopic studies, respectively. Maximum instrument resolution was ca. 0.8 cm^{-1}.

II. Assessments of Results

(1) Summary of Spectral Properties of *s*-Tetrazine in a Benzene Matrix. Optically good single crystals of *s*-tetrazine in benzene at 10^{-3} to 10^{-5} M were used for our absorption studies at 4.2 K. These crystals were dichroic and exhibited sharp zero phonon lines (ca. 1.0 cm^{-1}). A typical spectrum is shown in Figure 1. The assignments for the lines are based on our previous work in other mixed crystals[4] and the earlier study of benzene mixed crystals by Meyling, van der Werf, and Wiersma.[5] There is just one prevalent absorbing and emitting site having a 0–0 transition at 17 233.9 cm^{-1} corresponding to an out-of-plane polarized transition. The main part of the absorption is associated with the 702-cm^{-1} progression (6a). Isotopic zero-point shifts were measured at high spectral resolution. The line widths were close to 1 cm^{-1} with the 0–0 transitions at 17 236.9 cm^{-1} (^{15}N), 17 237.5 cm^{-1} (^{13}C), and 17 241.7 cm^{-1} (D). A spectrum of the 0–0 region is shown in Figure 2. These zero-point isotope shifts are all small compared with the displacement of the one-phonon sideband peak (~40 cm^{-1}) so there is very small overlap of these isotopic spectra and the isotopically scrambled phonon-sideband absorption. The compilation of isotopic data is given in Table I. It should be noted that the isotope shifts are often considerably larger in the region of vibronic bands than in the region of 0–0 bands.

Table I. Isotopically Selective Vibronic Spectra of Tetrazine in Benzene at 1.6 K

Assignment	Obsd zero-point energies and vibrational frequencies (vacuum cm^{-1})			
	$H_2C_2N_4$	^{15}N	^{13}C	D
6a″	727.3	723.2	720.2	717.9
0-0	17 233.9	17 236.9	17 237.5	17 241.7
2 × 16a′	532.6	529.0	531.2	
6a′	702.5	695.3	683.9	677.2
1′	806	809	813	
2 × 16b′	824	821	818	

The data in Table I come from experiments on these isotopes in natural abundance. The upper state vibrational assignments to specific vibrational state modes of tetrazine must be considered tentative since most of them are not observed in the fluorescence spectrum.

Fluorescence of *s*-tetrazine in benzene at 4.2 and 1.6 K was detected photoelectrically following a dye laser excitation at 5576 Å. The fluorescence spectrum, scanned with 1.0-cm^{-1} resolution, exhibits sharp zero phonon lines and a near-mirror image relationship to the absorption spectrum. Fluorescence is the unique emission following singlet excitation in the condensed[4,5] and gas[3,18] phases. There was no observable phosphorescence, unusual for azines in the condensed phase where intersystem crossing has been frequently invoked as the predominant photophysical pathway. The prominent emission feature is the 6a progression peaking at $6a_1^0$ and with $\nu_{6a''}$ = 727 cm^{-1}. Only one other ground state vibration is observable above the background noise. This vibration energetically matches 2 × 17b at 1853 cm^{-1}, and it also originates a progression in 6a″. A spectrum of fluorescence is shown in Figure 3, again in agreement with the results of Meyling, van der Werf, and Wiersma.[5]

(2) The Actual and Natural Radiative Lifetime of $^1B_{3u} \rightarrow {}^1A_g$. The literature contains conflicting reports of the lifetime τ_0 based on the integrated absorption, and since previous workers[12,17,18] were apparently not aware of the photochemical instability of *s*-tetrazine we have remeasured τ_0 in benzene solution at 300 K. The spectrum still displays 6a mode structure in fluorescence and absorption under these conditions. The absorption peaks at $6a_0^1$ (λ_{max} 5340 Å, ϵ_{max} 698); the higher energy state is structureless (λ_{max} 2767 Å, ϵ_{max} 313) and there is even stronger absorption as the benzene-like $\pi\pi^*$ region is approached.[14] The fluorescence and absorption $^1B_{3u} \rightleftarrows {}^1A_g$ involve mainly a_g modes so the method of Strickler and Berg[19] is applicable to determine τ_0. Taking the mean fluorescence wavelength at 5716 Å for $S_1 \rightarrow S_0$ and 3333 Å for the 3000 Å transition the calculated values of τ_0 are:

$$\tau_0(^1B_{3u} \rightarrow {}^1A_g) = 4.0 \times 10^{-7}\ s$$

$$\tau_0(3000\ Å) = 1.2 \times 10^{-7}\ s$$

Of course it is well known that the fluorescence yields are very small for each of these transitions. We have also measured the actual fluorescence lifetime of *s*-tetrazine in benzene solution using picosecond laser techniques.[20] The result obtained for τ_f was 450 ± 55 ps. The fluorescence quantum yield is therefore 1.1 × 10^{-3}, and since no measurable production of triplet states occurs subsequent to visible light absorption we conclude that the maximum photochemical yield is 0.999. The efficiency of internal conversion to the ground state is not known, though it is known[2,5] that the photochemical yield is of order unity.

The phosphorescence $^3B_{3u} \rightarrow {}^1A_g$ can be excited by direct optical pumping of the triplet state.[4,18] The 0-0 band occurs at 14 096 cm^{-1} and the lifetime of the neat crystal emission

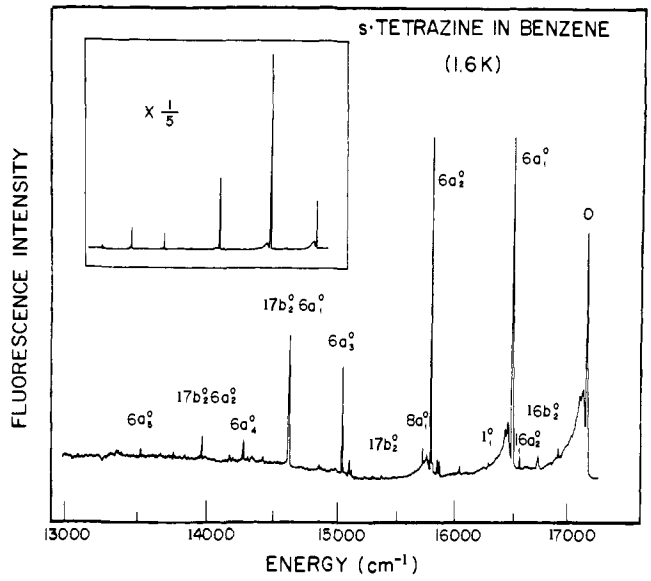

Figure 3. The fluorescence spectrum of *s*-tetrazine in benzene at 1.6 K. The fluorescence following dye laser excitation at 5576 Å was photoelectrically detected with 1-cm^{-1} resolution using a Spex scanning monochromator.

is 96.8 ± 2.1 μs. Thus we see that the process depleting singlet states occurs 2.1 × 10^5 times faster than that depleting the triplets. The existence of such a ratio strongly suggests that the depleting process is spin selective and that a spin-orbit interaction is needed to bring about depletion of triplets. Such a disparity between singlet and triplet decay times is not unusual when the depleting process is a radiationless transition such as internal conversion. In the present situation however it is likely that the dominant path of decay is photochemical (see below).

(3) Wavelength Dependence of Quantum Yield. The dye laser induced fluorescence of *s*-tetrazine in neat and mixed crystals at 4.2 and 1.6 K always originated from the vibrationally relaxed $^1B_{3u}$ state, regardless of the wavelength of excitation, and the fluorescence lifetime was always observed to be shorter than the dye laser pulse width of 5 ns, in agreement with our findings for the fluorescence lifetime in benzene solution (see above). For the lower lying vibronic levels it was certainly possible to excite essentially single levels using the dye laser and to search for emission at higher energy than the 0-0 region; since there was no hot luminescence it is apparent that for these vibronic levels the vibrational relaxation was occurring considerably faster than the 0-0 fluorescence rate, photochemistry, or internal conversion to the ground state. We have measured the relative quantum yield of fluorescence as a function of excitation energy in a mixed crystal at 1.6 K with up to 3000 cm^{-1} in excess of the 0-0 transition energy. This was done by comparing the intensities of the 6a progression members in excitation with those found in absorption. The result (shown summarily in Figure 4) that absorption and excitation profiles are very similar indicates that any increased rate of the photochemical process caused by increasing the energy excess is insufficient for the photochemical and vibrational relaxation rates to have become comparable. This same independence of the emission intensity (normalized to unit absorption) on excitation energy was observed in the triplet manifold up to an energy of 2200 cm^{-1} in excess of the 0-0 transition in the neat crystal.

(4) Isotopically Selective Vibronic Spectra. Isotopically selective absorption, fluorescence excitation, and fluorescence spectra were recorded for *s*-tetrazine in benzene at 1.6 K. Absorption lines in the region of the origin were measured with

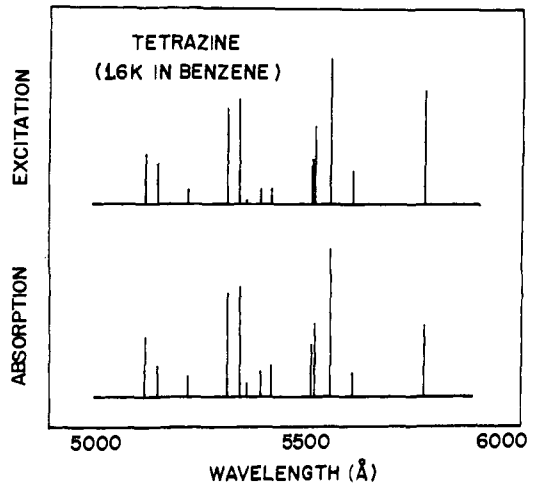

Figure 4. Comparison of the relative absorption and fluorescence excitation profiles of the singlet-singlet transition of *s*-tetrazine in benzene at 1.6 K. The absorption spectrum was photographed with a 3-m Baird spectrometer using a Xe continuum. The fluorescence excitation spectrum was recorded photoelectrically by monitoring the total fluorescence while scanning through the $^1B_{3u}$ absorption region with a N_2-pumped tunable dye laser. The excitation spectrum is normalized to the dye laser output.

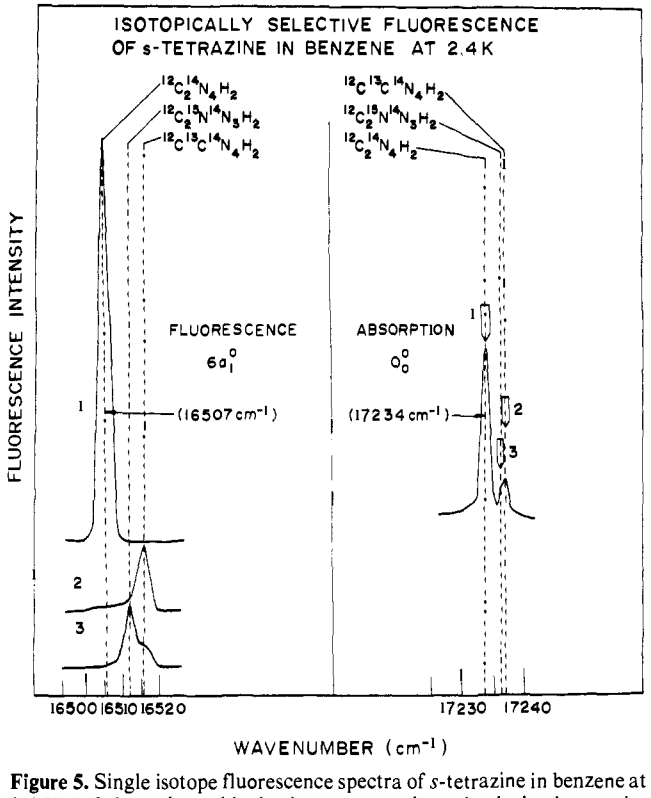

Figure 5. Single isotope fluorescence spectra of *s*-tetrazine in benzene at 2.4 K. A 0.6-cm^{-1} tunable dye laser was used to selectively photoexcite a single isotopic species of *s*-tetrazine (as shown by the numbered arrows). The resulting fluorescence spectra were obtained photoelectrically using a Spex scanning monochromator.

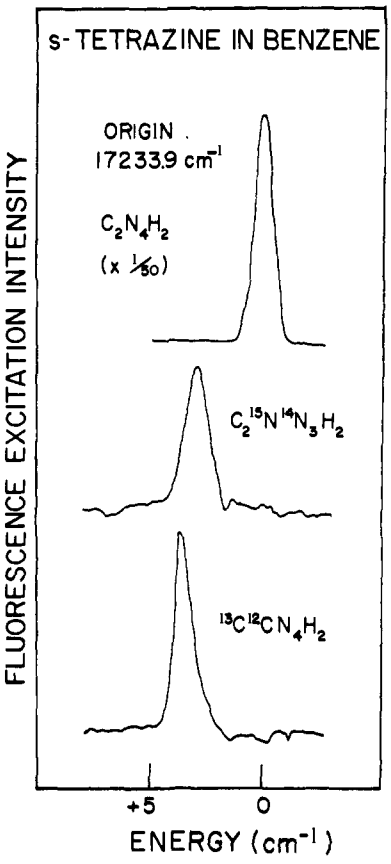

Figure 6. Single isotope fluorescence excitation spectra of *s*-tetrazines in benzene at 1.6 K. A Spex scanning monochromator with 0.8-cm^{-1} resolution was tuned to the fluorescence wavelength of a single specific isotope of *s*-tetrazine. The 0.6-cm^{-1} tunable dye laser output was then scanned through the absorption region and the excitation spectrum recorded photoelectrically.

0.5 cm^{-1} resolution and identified as normal, ^{15}N-, and ^{13}C-tetrazine from their relative peak intensities. Excitation spectral studies of native (nonenriched) *s*-tetrazine in mixed crystals, suitably dilute to avoid saturation effects, confirmed the spectral distinctions between molecules containing one atom of each of these two isotopic species as well as monodeuteriotetrazine, with relative intensities expected from the natural isotopic abundances (100:2.3:1.7:0.05 = $^{12}C_2{}^{14}N_4H_2$:$^{13}C^{12}C^{14}N_4H_2$:$^{12}C_2{}^{15}N^{14}N_3H_2$:$^{12}C_2{}^{14}N_4HD$). These experiments provide conclusive identification of the isotopic species being observed, and further indicate that there are no noticeable isotope effects on the photochemical reaction processes.

Dye laser excitation of a single isotopic species resulted in fluorescence exclusively from the particular single isotope originally excited. There was no evidence of any isotopic scrambling between excitation, vibrational relaxation, and subsequent electronic relaxation. Single isotopic species fluorescence, detected at ca. 0.8 cm^{-1} resolution, was used to identify the isotopic $^1B_{3u} \rightarrow {}^1A_g$ origins and progressions of 6a. Figure 5 shows single isotope fluorescence spectra in the $6a_1{}^0$ region. The $\nu_{6a''}$ vibrational frequency is 727.3, 723.2, 720.2, and 717.9 cm^{-1} for normal and monosubstituted ^{15}N-, ^{13}C-, and D-tetrazine, respectively (see Table I).

By monitoring fluorescence at a frequency characteristic of a single selected isotopic tetrazine the isotopically selective excitation spectra were obtained. The single isotope fluorescence excitation spectra of the origin are shown in Figure 6. The vibrational frequencies obtained through this isotopically selective fluorescence study are presented and assigned in Table I. Broad band detection of the excitation spectrum in Figure 2 indicates the extent of the spectral overlap of the various isotope transitions. Most of the observed overlapping is the result of inhomogeneous line broadening, only a small amount arises from a coincidental compensation of zero-point energy and vibrational frequency shifts. Isotopically selective stimulation of photoprocesses, such as luminescence or a primary chemical reaction, was readily achieved by choosing the excitation wavelength to correspond to a vibronic region where the desired isotopic species were better resolved than in the 0-0

Table II. *s*-Tetrazine in Benzene Singlet Excitation Spectra at 1.6 K

Tetrazine lines			
Position (vacuum cm^{-1})	Rel inten	Interval (vacuum cm^{-1})	Assignment
17 234	s	000	Origin
17 615	w	381	$6b_0^1$
17 766	m	532	$16a_0^2$
17 813	w	579	a
17 840	w	606	b
17 892	mw	658	c(ν_4)
17 936	vs	702	$6a_0^1$
17 938	vw	704	$17b_0^1$
18 040	ms	806	1_0^1
18 058	ms	824	$16b_0^2$
18 209	w	975	d(5, 10b)
18 236	mw	1002	$(8a, 9a)_0^1$
18 284	w	1050	e(3, 9b)
18 320	w	1086	$6b_0^1\ 6a_0^1$
18 373	mw	1139	f
18 394	mw	1160	a_0^2
18 461	mw	1227	$16a_0^2\ 6a_0^1$
18 515	w	1281	a $6a_0^1$
18 524	w	1290	h (8b)
18 542	w	1308	b $6a_0^1$
18 594	w	1360	c $6a_0^1$
18 634	vs	1400	$6a_0^2$
18 643	s	1409	$17b_0^2$
18 737	vs	1503	$1_0^1\ 6a_0^1$
18 755	m	1521	$16b_0^2\ 6a_0^1$
18 890	w	1655	i
18 910	w	1676	d $6a_0^1$
18 921	w	1687	j
18 935	w	1701	$(8a, 9a)_0^1\ 6a_0^1$
18 975	w	1741	c $6a_0^1$
19 014	w	1780	$6b_0^1\ 6a_0^2$
19 074	m	1840	f $6a_0^1$
19 095	w	1861	$a_0^2\ 6a_0^1$
19 166	mw	1932	$16a_0^2\ 6a_0^2$
19 214	w	1980	a $6a_0^2$
19 228	w	1994	h $6a_0^1$
19 241	w	2007	b $6a_0^2$
19 314	w	2080	c $6a_0^2$
19 330	m	2096	$6a_0^3$
19 338	mw	2104	$16b_0^2\ 6a_0^2$
19 434	s	2200	$1_0^1\ 6a_0^2$
19 452	mw	2218	$16b_0^2\ 6a_0^2$
19 582	w	2348	i $6a_0^1$
19 604	w	2370	d $6a_0^2$
19 628	w	2394	j $6a_0^1$
19 646	w	2412	$(8a, 9a)_0^1\ 6a_0^2$
19 663	w	2429	
19 686	w	2452	e $6a_0^2$
19 752	w	2518	
19 795	w	2561	f $6a_0^2$
19 871	w	2637	$16a_0^2\ 6a_0^3$
19 899	w	2665	a $6a_0^3$
20 023	w	2789	c $6a_0^3$
20 035	mw	2801	$6a_0^4$
20 043	w	2809	$17b_0^2\ 6a_0^2$
20 139	mw	2905	$1_0^1\ 6a_0^3$

region. Table II gives a complete survey and analysis of the transitions seen by means of excitation of *s*-tetrazine in benzene.

(5) Isotope Separations. The photochemical instability of *s*-tetrazine combined with the chemically stable nature of the photoproducts (see below) makes this a most suitable system for laser-induced isotope enrichment.[2a] We have performed selective irradiation experiments on dilute mixed crystals at

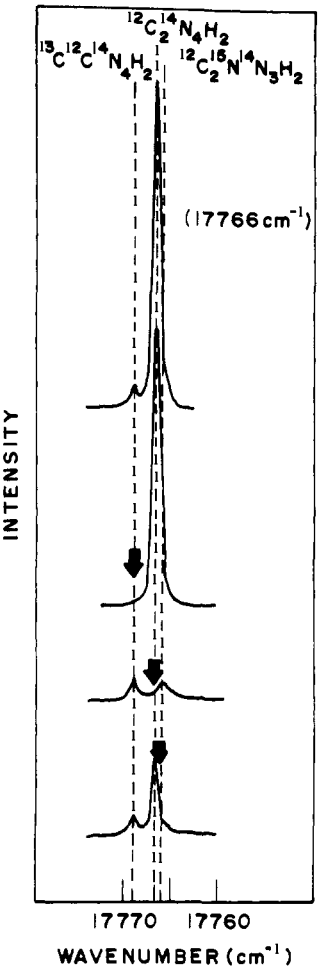

Figure 7. Excitation spectra of the isotopically selective photodecomposition of *s*-tetrazine in benzene at 1.6 K. Excitation and photolysis source was a 0.6-cm^{-1} N_2-pumped tunable dye laser. Four suitably dilute crystals showing the natural abundances of ^{13}C- and ^{15}N-containing tetrazine in benzene were used. Transition energies for each isotopic species of tetrazine were established in the first sample. Each subsequent sample was irradiated at a specific isotope transition as indicated by the arrows. Subsequent low-intensity dye laser excitation spectra demonstrate the high degree of isotopic selectivity achieved in the decomposition reaction by this method.

1.6 K and achieved separation factors in the range 10^4. The starting material was natural *s*-tetrazine in all cases.

The experiments were performed in the manner of the excitation spectra (III.4) except that the wavelength scan was stopped when the transition energy for a particular isotope was reached. The best excitation frequency could be ascertained quite readily either by monitoring the total emission and settling on a particular peak, or by fixing the detector monochromator at a known emission frequency for one of the isotopes and maximizing the fluorescence signal at the detector during a dye laser scan. Finally when the optimum settings of the dye laser are known it is possible to initiate the irradiations of fresh material with the required excitation wavelength. Figure 7 shows the excitation spectra of the $16a_0^2$ transition for different crystal samples that had experienced no previous irradiation. A dye laser having a 40× beam expander was used for these irradiations and its line width was 0.6 cm^{-1}. The excitation spectra in Figure 7 were recorded with a very low intensity beam after the irradiation so the spectra represent the situation existing after the isotopically selective irradiation, and they leave no doubt that an effective separation was obtained for ^{13}C, ^{15}N, and ^{12}C and ^{14}N. We have not spectrally identified molecules of *s*-tetrazine containing two atoms of ^{13}C, or two atoms of ^{15}N, or one atom of ^{13}C with one of ^{15}N. These

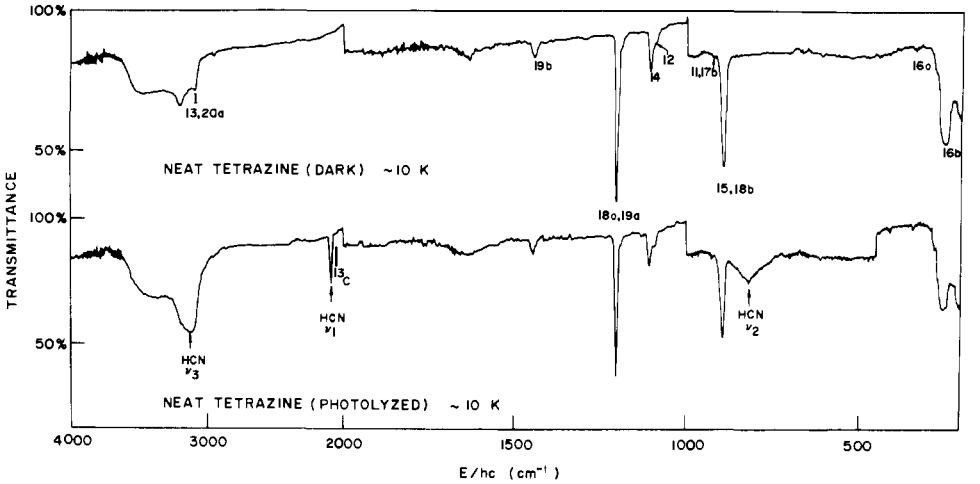

Figure 8. Infrared spectra of neat *s*-tetrazine and of tetrazine photolysis products at 10 K. Photolysis source was a 1000 W Xe lamp filtered to pass 5800 Å > λ > 4500 Å.

three types of molecules have abundances of 2.4×10^{-4}, 1.6×10^{-4}, and 3.3×10^{-4}, respectively. Since it is not difficult to calculate where the spectra of these molecules are expected to be located these need not represent the limit of achievable isotope separation. For example, in the present experiments the monodeuteriotetrazine spectrum is not readily observed in the absorption or excitation spectra. However, by detecting fluorescence through a monochromator fixed at an appropriate wavelength to discriminate proto and deuterio molecules, the presence and photochemical destruction of the deuterated molecule is easily established.

(6) Photochemistry of *s*-Tetrazine. Though there have been repeated reports[12,17,18] of the absence of photochemistry following long wavelength excitation of *s*-tetrazine, it was recently shown[2,4,5] that indeed an extremely efficient photochemical reaction does occur. It is trivial to demonstrate that *s*-tetrazine rapidly disappears when crystals, mixed crystals, solutions, or the gas are irradiated, since after just a few minutes of exposure to the dye laser the samples, originally deep red, become colorless. We have undertaken low-temperature infrared and Raman spectral studies to identify the primary products in the photochemistry of the singlet and of the triplet B_{3u} states. We have also studied the products following uv excitation. The separation of *s*-tetrazine isotopes in the gas phase was recently reported.[21]

The infrared spectra of neat and photolyzed tetrazine films were observed at 10 and 4.2 K on a Perkin-Elmer 225 infrared spectrometer using CsI dewar windows. All allowed infrared active modes of tetrazine were observed and assigned from previous vibrational studies.[2b,22] The only contamination observable in the neat films was slight amounts of water. Selective irradiation of the T_1, S_1, and S_2 states was achieved by using a 1000 W Xe arc with filtration for 7500 Å > λ > 6000 Å, or 5800 Å > λ > 4500 Å, or a high-pressure Hg arc with a uv interference filter, λ_{max} ~2800 and 300 Å band pass, respectively. The irradiation was focused directly into the sample through a quartz window. A 30 cm water filter was used to remove ir from the photolysis source. In all instances only small fractions of the neat tetrazine films were photolyzed to avoid possible reactions between excited tetrazine and its photoproducts.

The results of all the photolysis experiments were the same. Figure 8 shows the spectral changes upon partial photolysis and Table III lists the observed vibrational energies. Only one infrared active photoproduct was observed at 4.2 K; increase in activity at 819, 2060, 2092, and 3125 cm^{-1} can be assigned to HCN (and $H^{13}CN$). Although some of the infrared activity in the region of 3000 to 3500 cm^{-1} is indicative of water contamination, the notable decrease in this broad absorption region upon irradiation of a neat tetrazine film indicates substantial hydrogen bonding in neat tetrazine. On warming the sample to 77 K, N_2 was distilled off and detected by a pressure gauge. No other volatile gases were detected.

Table III. Low-Temperature Vibrational Spectra of Neat Tetrazine and Its Photolysis Products

	Assignment	
E/hc, cm^{-1}	Tetrazine	Photoproducts
Raman (1.6 K)		
663 ± 3	$6b(b_{3g})$	
737	$6a(a_g)$	
795	$4(b_{2g})$	
1011	$5, 1(b_{2g}, a_g)$	
1301	$3(b_{3g})$	
1424	$8b(b_{3g})$	
1526	$8a, 9a(a_g)$	
2130		HCN (CH stretch)
2360		N_2
3095	$2(a_g)$	
Infrared (4.2 K)		
250	$16b(b_{1u})$	
338	$16a(a_u)$	
819		HCN (degenerate bend)
893	$15, 18b(b_{1u})$	
925	$11, 17b(b_{3u})$	
1095	$12(b_{2u})$	
1107	$14(b_{3u})$	
1203	$18a, 19a(b_{2u})$	
1448	$19b(b_{3u})$	
2060		$H^{13}CN$(CN stretch)
2092		HCN
3090	$13, 20a(b_{2u})$	
3125		HCN (CH stretch)

The Raman scattering of *s*-tetrazine and the photolysis products was studied at 1.6 K in the neat and mixed crystals at various excitation frequencies. Direct confirmation of the photoproducts and a preresonance scattering enhancement effect were obtained. All Raman spectra were obtained with a Spex Ramalog 1401, coupling a tunable Ar^+ laser with a double Spex and using photon counting detection with a cooled Ga-As photomultiplier. The three systems studied are the neat crystal and mixed crystals at 1.6 K and solutions at 300 K. In all instances, when the excitation frequency was higher than the S_1 origin, fluorescence dominated any Raman scattering by several orders of magnitude. Raman scattering following

excitation in the triplet manifold in low-temperature solids was comparable in magnitude with the phosphorescence intensity.

The observed tetrazine and photoproduct Raman transitions are tabulated in Table III. All g vibrational modes of tetrazine were observed and assigned from previous work.[16] Neat crystals at 1.6 K were irradiated by the 5308-Å Ar^+ line and then the 5682-Å Raman scattering was observed. Increases in Raman intensity corresponding to vibrational energies of 2129 and 2358 cm^{-1} singularly identify HCN and N_2 as the predominant low-temperature primary products of this efficient, photochemical decomposition of *s*-tetrazine.

A preliminary examination of relative vibrational scattering cross sections as a function of excitation energy showed dramatic preresonance effects. The scattering from the 5682- and 6471-Å Ar^+ lines is shown in Figure 9. These were the only usable lines for Raman studies; the other available lines fell within the singlet manifold and produced overwhelming fluorescence signals. The line at 6471 Å (15 454 cm^{-1}) is nearly coincident with a medium strength triplet vibronic band with b_{3g} vibrational symmetry. There is an accompanying, and dramatic, increase in the relative intensities of the observed b_{3g} Raman vibrational transitions as compared with the 5682-Å Raman spectrum. The latter shows a Franck-Condon intensity pattern similar to the $^1B_{3u} \leftarrow {}^1A_g$ electronic transition.

In summary these studies show that at low temperatures in these mixed crystals only HCN an N_2 are seen to be produced following irradiation of *s*-tetrazine in any of the aforementioned spectral regions. The strengths of the bands seen in the spectra indicate that the production of these species is quantitative. Subsequent mass spectral analysis of the photoproducts from irradiated gaseous tetrazine conclusively demonstrated that the photochemical yield is 2:1 = HCN:N_2.

(7) Thermochemistry of *s*-Tetrazine. *s*-Tetrazine vapor undergoes a thermal decomposition at room temperature in the dark and HCN is a prevalent product of the thermal reaction also. Our studies of the vapor in equilibrium with the solid at 320 K showed that HCN was the only significant infrared active reaction product.

The thermochemistry of the process:

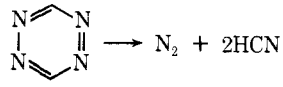

was estimated by extrapolating combustion data available for other azines.[22] We find an enthalpy of -1 kcal mol^{-1} for the ground state reaction. The singlet photoreaction is therefore expected to have an exothermicity of greater than 60 kcal mol^{-1}. It is well within the expected accuracy of this estimate to regard the electronic transition energy as a first approximation to the exothermicity of the photoreaction. Thus there is reason to believe that in the photoreaction HCN and N_2 will be formed in vibrationally excited states.

IV. Discussion

The photodissociation of *s*-tetrazine does not involve any intermediates that are stabilized at 1.6 K for an appreciable time. This is to be contrasted with the gas phase photodissociation of pyridazine which is claimed to produce in high yield the diethynyl radical and nitrogen.[6,23] Although Chapman and co-workers[24] have identified hitherto unobserved intermediates at 77 K and in inert gas matrices at 8 K, the overall effects of rigid molecular crystal lattices at 4.2 to 1.6 K on reaction yield and direct product stabilization have not been fully explored.

(1) Characteristics of Low-Temperature Crystal Spectra in Relation to Isotope Separations. There are several factors that

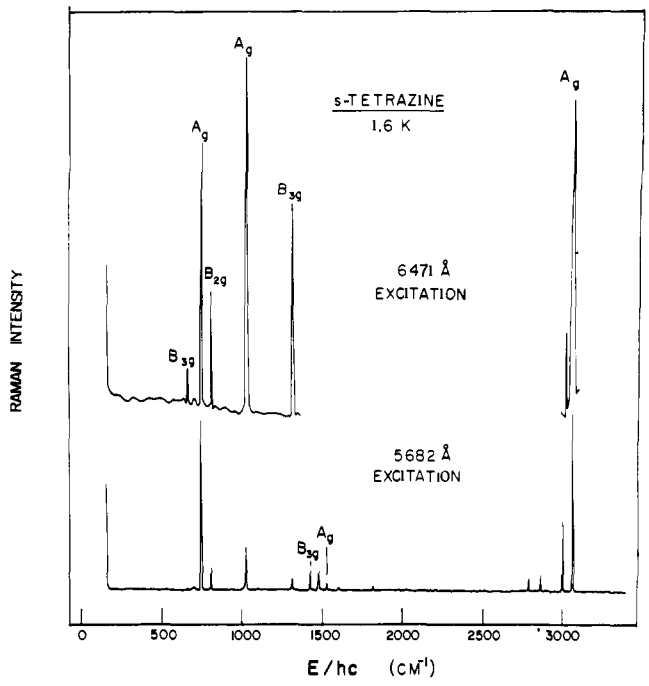

Figure 9. Raman spectrum of neat *s*-tetrazine at 1.6 K. The spectra were photoelectrically recorded with a Spex double monochromator and photon counting using various lines of an Ar^+ laser. E/hc is measured from the laser position. The upper spectrum is resonance enhanced by the triplet state.

contribute to the observed linewidth of crystal spectra. The smallest of these involves the interaction of the chromophore with the radiation field. Even for strong transitions the radiative frequency width is less than 10^9 s^{-1} corresponding to an energy uncertainty of 0.03 cm^{-1}. Excited vibronic states experience varying degrees of broadening due to irreversible intramolecular nonradiative couplings to vibronic levels of lower lying electronic states and the lattice phonon modes. These homogeneous, nonradiative line broadening processes include vibrational relaxation to the zero point of a given electronic state, internal conversion to a lower lying electronic state with the same spin, and intersystem crossing to lower electronic states of different multiplicity. There is further nonradiative broadening due to predissociation and photoinduced chemical reactivity.

The predominant contribution to the observed line width is the energetically inhomogeneous distribution of sites within the crystal. In random solids such as glasses at 77 K this distribution may easily span more than 100 cm^{-1}. In mixed crystals and neat crystals at 4.2 K the inhomogeneous line width is in the range of 3.0 to 0.1 cm^{-1}. Although there is no rotational congestion in condensed phase spectra, there is a weak semistructured sideband associated with each sharp molecular transition. This sideband arises from a coupling of the chromophore with the crystal lattice allowing absorption of photons with energies greater than the molecular transition energy. This excess energy is dissipated into allowed lattice modes. In many heteroaromatics these phonon bands are very weak and the peaks are well removed from the sharp zero-phonon band. The spectral overlap of naturally abundant isotope phonon sidebands and the rare isotope zero-phonon bands may represent the upper limit of selectivity of a single isotopic excitation scheme. We can represent the strength of the coupling with phonons in terms of the relative intensities of the zero-phonon transition and the phonon sideband. To a first (and often useful) approximation the phonon sideband is represented by $I_p(\omega/\omega_D)^2$ where ω_D is the (peak) cut-off frequency, at which point the absorption intensity is I_p, and

ω is measured from the zero-phonon line. Then ω_i is the isotope shift ($\omega_i \ll \omega_D$), α is the abundance of a heavier isotope, and W is the ratio of phonon sideband to zero-phonon line integrated absorption intensities, the initial optical discrimination between light and heavy isotopes for a narrow band excitation is:

$$\left[1 + \left(\frac{3}{\alpha}\right)\left(\frac{\omega_i}{\omega_D}\right)^2 W\left(\frac{\Delta\omega_0}{\omega_D}\right)\right]^{-1}$$

Thus when either the isotope shift is extremely small or when the zero-phonon line (width $\Delta\omega_0$, peak intensity I_0) is strong compared with the phonon sideband peak, the discrimination factor will remain close to unity, and nearly perfect isotope separation will be possible. In many molecular crystals $(\Delta\omega_0/\omega_D) \simeq 1/50$, $(\omega_i/\omega_D)^2 \simeq 1/100$, and W ranges from 0.01 (very weak excitation phonon coupling) to ~100 for strong phonon interactions. Thus for carbon-13 where α is made up from 0.01 for each carbon atom in the molecule, and $I_p/I_0 = 0.1$ (moderately weak coupling), the discrimination factor is 0.9998. In many mixed crystals at low temperatures molecules with a specific isotopic substitution at various different atomic positions can be optically discerned. Therefore an important application might be to use laser photoselection in solids to produce small quantities of molecules having highly specialized isotopic substitutions.

(2) Spin Selectivity of the Photoreaction. The absorption of visible light by *s*-tetrazine does not provide sufficient energy to generate excited states of the N_2 or HCN products. It follows that the reaction must proceed through singlet states. An additional evidence for this model derives from the observed spin selectivity of the photochemical process. We have measured[4] the triplet lifetime to be 97 μs and ascertained that the dominant mode of triplet decay is predissociation into products HCN and N_2. The fluorescence lifetime of 450 ps is also determined by the photochemical reaction. The gas phase phosphorescence lifetime[18] is 72 μs, and the fluorescence lifetime for the zero-point level of $^1B_{3u}$ in the gas has been shown[25] to be in the range of 850 ps. An important conclusion is that both in the gaseous and solid phases the photochemical reaction occurs nearly 10^5 times more effectively from the singlet than from the triplet state of *s*-tetrazine. The total energy content in the equilibrated singlet is 4318 cm^{-1} in excess of the equilibrated triplet. Conceivably this energy excess could make some difference to the predissociation rate. On the other hand there was no change in the relative quantum yield of phosphoresence following excitation over the range 2200 cm^{-1} to higher energy than the zero-point level of the triplet state. An indication that we draw from these facts is that the reaction may not proceed through a biradical intermediate (such as that produced by splitting off N_2 from *s*-tetrazine). Such a biradical would have nearby singlet and triplet states, and so there would not be expected a large difference in the predissociation for $^1B_{3u}$ and $^3B_{3u}$ due to spin. It is difficult to assess the importance of the energy discrepancy (singlet-triplet splitting) and clearly low-pressure triplet-excitation studies are needed in order to clarify that question. On the basis of available data it appears likely that the $^3B_{3u}$ predissociation is spin-orbit induced. By this we mean that the photoreaction is occurring by virtue of the mixing of singlet states into the triplet state by spin-orbit coupling. The prohibition factor on dissociation from the triplet state of 10^{-5} is in the range of the usual ratios of singlet to triplet lifetimes in heteroaromatic molecules. In making such comparisons, however, it should be considered that *s*-tetrazine appears to function closer to a statistical limit than the other azines. If, in a zeroth-order approximation, it is assumed that the $^1B_{3u}$ and $^3B_{3u}$ predissociations involve similar final densities of states and vibrational overlap factors then the relative rates in a statistical model would be given by:

$$k_T/k_S = |V_T/V_S|^2 \cong |a_{ST}|^2$$

where $|a_{ST}|^2$ is the probability of measuring a singlet component in the triplet state. The a_{ST} is one of the same factors that cause radiative transitions to and from triplet states. Thus $|a_{ST}|^2$ is approximately the ratio of the observed radiative rates for triplet-singlet and singlet-singlet transitions. Since tetrazine is centrosymmetric there is no possibility that the zero-point state of $^3B_{3u}$ can be directly spin-orbit mixed with the ground state. On the other hand vibrational levels of the ground state nearby to $^3B_{3u}$ and having the proper spin-orbit symmetries (i.e., B_{2u}, B_{1u}, or A_u) may couple with one or another of the three spin sublevels while the molecule undergoes nuclear displacements along the appropriate normal modes (i.e., b_{2u}, b_{1u}, or a_u modes, respectively). It is by such a mechanism that the spin-orbit-induced predissociation might proceed through the intermediary of the vibrational levels of the ground state. It is obvious that the predissociation may therefore be occurring at different rates from different spin-sublevels of the triplet state and experiments are underway to test this motion. For a more exact description of the predissociation of *s*-tetrazine one would need to take into account the details of the quasi-continuum level structure in the neighborhood of the singlet and triplet states. The triplet state energy of *s*-tetrazine is actually only about 75% of the singlet state energy and this may introduce significant differences in the predissociation rate over and above the electronic factor.

Acknowledgment. We thank Dr. Amos B. Smith III for valuable discussions of this work.

References and Notes

(1) This research was supported in part by an NIH Grant GM12592 and in part by the NSF/MRL at the University of Pennsylvania.
(2) (a) R. M. Hochstrasser and D. S. King, *J. Am. Chem. Soc.*, **97**, 4760 (1975); (b) R. M. Hochstrasser and D. S. King, "Lasers in Physical Chemistry and Biophysics", Elsevier, Amsterdam, 1975.
(3) A. E. W. Knight and C. S. Parmenter, *J. Lumin.*, in press.
(4) R. M. Hochstrasser and D. S. King, *Chem. Phys.*, **5**, 439 (1974).
(5) J. H. Meyling, R. P. van der Werf, and D. A. Wiersma, *Chem. Phys. Lett.*, **28**, 364 (1974).
(6) J. R. Fraser, L. H. Low, and N. A. Weir, *Can. J. Chem.*, **53**, 1456 (1975).
(7) M. Kasha, *Discuss. Faraday Soc.*, **No. 9**, 14 (1950).
(8) K. K. Innes, J. P. Byrne, and I. G. Ross, *J. Mol. Spectrosc.*, **22**, 125 (1967).
(9) Th. Curtius, A. Darapsky, and E. Muller, *Ber.*, **40**, 84 (1906).
(10) J. Koenigsberger and K. Vogt, *Phys. Z.*, **14**, 1269 (1913).
(11) G. H. Spencer, Jr., P. C. Cross, and K. B. Wiberg, *J. Chem. Phys.*, **35**, 1925 (1961).
(12) A. J. Merer and K. K. Innes, *Proc. R. Soc., London, Ser. A*, **302**, 271 (1968).
(13) D. T. Livak and K. K. Innes, *J. Mol. Spectrosc.*, **39**, 115 (1971).
(14) S. F. Mason, *J. Chem. Soc.*, 1240 (1959).
(15) M. Chowdhury and L. Goodman, *J. Chem. Phys.*, **36**, 548 (1962).
(16) W. D. Sigworth and E. L. Pace, *J. Chem. Phys.*, **54**, 5379 (1971).
(17) G. K. Vemulapalli and T. Cassen, *J. Chem. Phys.*, **56**, 5120 (1972).
(18) J. R. McDonald and L. E. Brus, *J. Chem. Phys.*, **59**, 4966 (1973).
(19) S. J. Strickler and R. A. Berg, *J. Chem. Phys.*, **37**, 814 (1962).
(20) R. M. Hochstrasser, D. S. King, and A. C. Nelson, *Chem. Phys. Lett.*, in press.
(21) R. R. Karl and K. K. Innes, *Chem. Phys. Lett.*, **36**, 275 (1975).
(22) A. Albert, "Heterocyclic Chemistry", 2d ed, Athione Press, London, 1968.
(23) We have examined the photolysis of pyridazine in a C_6H_6 lattice at 4.2 K. Under these conditions the apparent quantum yield is less than ca. 10^{-3}, assuming that the product is not pyridazine itself. N_2 is the only photoproduct conclusively identified.
(24) O. L. Chapman, P. W. Wojtkowski, W. Adam, O. Rodriguez, and R. Ruckstäschel, *J. Am. Chem. Soc.*, **94**, 1365 (1972); O. L. Chapman, K. Mattes, C. L. McIntosh, J. Pacansky, G. V. Calder, and G. Orr, *ibid.*, **95**, 6134 (1973).
(25) We are indebted to Dr. J. Langelaar, University of Amsterdam, for providing us with as yet unpublished data on the fluorescence lifetimes of single vibronic levels of *s*-tetrazine.